

# Combined DC/AC supply on a single distribution cable

Peter van Duijsen  
Simulation Research  
www.caspoc.com  
The Netherlands  
p.vanduijsen@casnoc.com

Wilfred Akerboom  
CityTec  
www.citytec.nl  
Alblasserdam, The Netherlands  
Wilfred.Akerboom@citytec.nl

Johan Woudstra  
THUAS  
www.hhs.nl  
Delft, The Netherlands  
j.b.woudstra@hhs.nl

**Abstract**—A commonly used low voltage power cable in The Netherlands has four main conductors for distribution and additionally four smaller sized conductors for powering public lighting or other services. This cable is called the combined-cable. In practice, two AC distribution grids are in parallel in a single distribution cable.

The four additional conductors can also be applied for a separate DC distribution grid for public LED street lighting. Cost reduction thanks to a reduced number of feed-in points, extension of life span by reusing existing cables and reduced cable power loss are the main arguments for a combined DC/AC distribution on a single cable. Increased reliability and safer earth-leakage detection and safer short-circuit detection are important aspects of a DC distribution for public lighting.

The research question is if the 400V, 3-phase AC grid can be combined into a single cable with regards to cross-talk and safety. A 2D electromagnetic model is set up to model the electromagnetic interactions in the cable. A circuit model based on the outcome of the electromagnetic model is set up and used in circuit simulation to test various conditions and behavior. For example, do AC disturbances and AC load steps in the AC grid influence the power electronics safety components in the DC grid. The simulation and measurement results indicate that the power electronics safety components in the DC grid are largely unaffected by transients in the AC grid. Simulation results are confirmed by the outcomes of first measurements.

**Index Terms**—Power Distribution, DC grid, Inductive coupling, simulation

## I. INTRODUCTION

In the AC distribution grid a commonly used low voltage power cable is the so called combined-cable, see Fig. 1. The cable has four main conductors for powering the houses and additionally four smaller sized auxiliary conductors powering public lighting or other services. In the Netherlands 2.3 million (67% of all) light poles are connected to the combined-cable. In the current situation the combined-cable is connected to alternating current (AC) supplies. Because of developments in the public lighting sector, for example the use of LED drivers and fixtures, the application of Direct Current (DC) as power supply is a new possibility, [4] [5]. Recent research [13], shows that DC is safer than AC because of the use of solid state safety relays. With those relays it is possible to detect and switch off a

fault in microseconds instead of milliseconds, [2], [3]. Further it is almost impossible to use earth-leakage detection with an AC supply, however in a DC grid earth-leakage detection is possible even for longer cable length. Because of this fault detection, a DC grid is safer with regard to accidents between cars and light poles and for construction and maintenance.

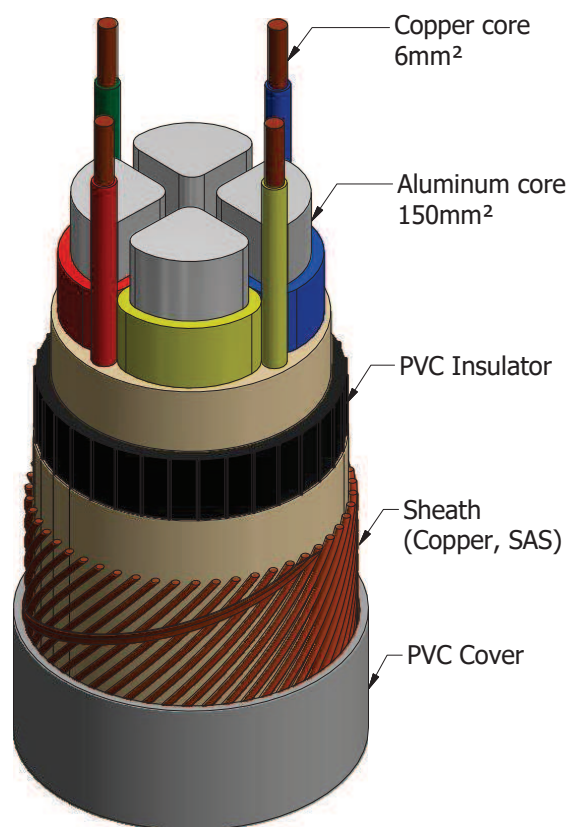


Fig. 1. Side view of the combined-cable [11], AC on the Aluminum  $150\text{mm}^2$  cores and DC over the copper  $6\text{mm}^2$  cores

Due to higher DC voltages (+350V and -350V), instead of AC 230V RMS, the cable capacity is increased by 52%.

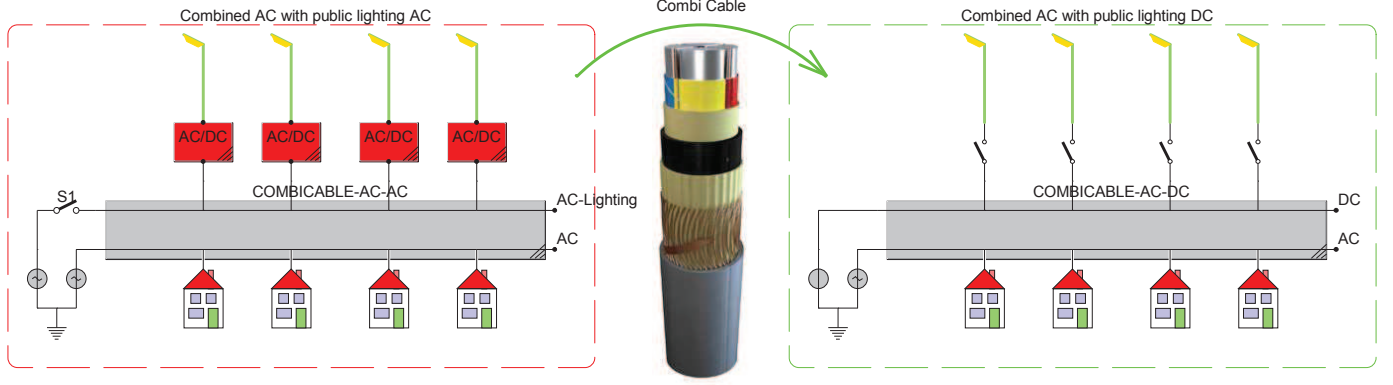


Fig. 2. Combined AC and DC on the combined-cable.

For an AC grid only two single phases using four cores were utilized, for the DC grid, three cores are utilized, making  $-350V \leftrightarrow 0V \leftrightarrow +350V$ . Because of the higher voltage but equal nominal current through the cores, the power is increased.

$$V_{AC}^{rms} = 230V \quad (1)$$

$$V_{DC} = 350V \quad (2)$$

$$P_{AC} = V_{AC}^{rms} \cdot I^{nominal} \quad (3)$$

$$P_{DC} = V_{DC} \cdot I^{nominal} \quad (4)$$

Therefore the power is increased by

$$\frac{P_{DC}}{P_{AC}} = \frac{V_{DC} \cdot I^{nominal}}{V_{AC}^{rms} \cdot I^{nominal}} \quad (5)$$

$$\frac{P_{DC}}{P_{AC}} = \frac{350}{230} = 1.52 \quad (6)$$

Another positive point is the fact that during a short-circuit fault, there are no maximum short-circuit currents because of the fast switching in case of faults. Because of all these advantages it is interesting to study the possibility to supply all public lighting systems with DC. In the case of the combined-cable it is interesting to investigate if it is possible to connect DC to the auxiliary conductors so that they can be used for powering DC-LED public lighting systems. Advantage in the combined-cable approach is that it is not necessary to use a separate cable for public lighting. The research question is: Can you work safely with the combined-cable when the distribution conductors are connected with an AC supply and the auxiliary conductors with a DC supply? In other words, can the two grids be combined into a single cable with regards to crosstalk and safety?

The use of an electromagnetic and simulation model of the combined-cable with all the mutual inductance and capacitance will be evaluated with help of transient measurements on the cable. These models will be used for circuit simulation tests for various conditions and behaviors.

## II. CONCEPTS

The main research question is if the AC and DC grid can be combined in a single cable. This principle is applied in today's public lighting. The idea is to move from AC public lighting towards DC public lighting, mainly because of costs and safety issues. The concept is displayed in Fig. 2. Within the red dashed area the current situation is displayed, where two AC grids are supported by the combined-cable. The public street lighting is switched on and off using the main switch S1. Wherever DC LED armatures are applied, a DC/AC converter is placed either in the pole or fixture.

When transitioning to a DC distribution as shown within the green dashed area in Fig. 2, both a DC and AC grid are combined within the same combined-cable. The AC distribution is remained for supplying the regular consumers like houses and offices, but the public street lighting supply is replaced by a DC grid.

A difference between the AC and DC distribution grid is that the AC distribution grid for public lighting is switched by the central switch S1 in Fig. 2, where in the DC distribution, each public lighting pole can be switched individually and the DC grid remains powered constantly. This allows other low-power devices to be connected to the DC grid, like remote sensors, surveillance cameras and public WIFI.

To study the implementation of a combined AC and DC distribution in a single cable, simulation studies are done and experimental setups are carried out. For the simulation studies a detailed simulation model of the combined-cable is required to model all voltage/current relations between the eight cores inside the combined-cable, [6], [7]. The simulation model is compared to an experimental set-up, [11], before the model is used in a case study.

First a simulation model is set up based on the electromagnetic coupling between the cores inside the cable. Those couplings are based on the cross-sections of the cores and the distance between them, see Fig. 5.

The datasheet [8] gives basic information on the parameters describing this cable. However, important parameters are missing from this datasheet, such as the inductive coupling between

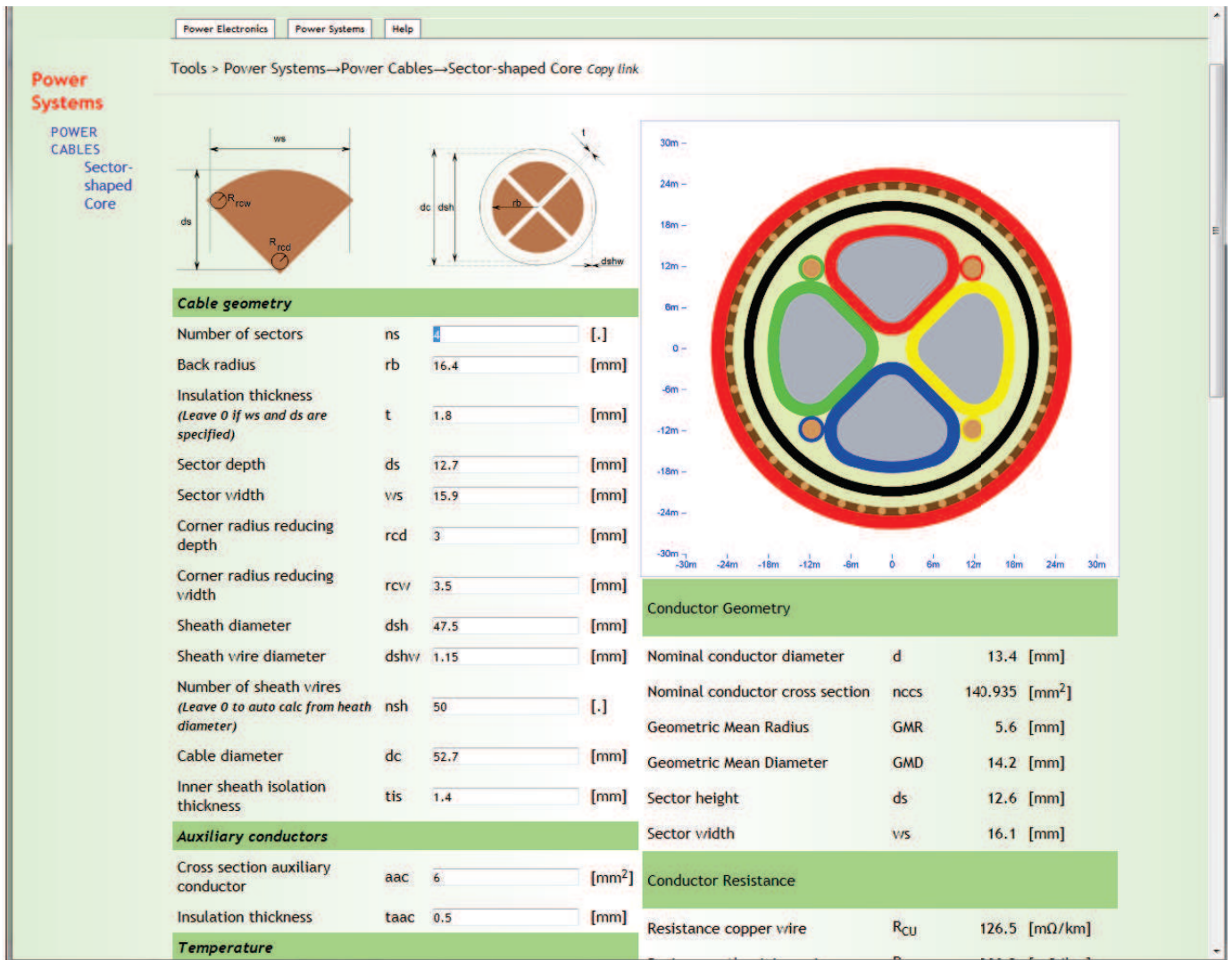


Fig. 3. Caspoc tool for calculating the electrical parameters of the combined sector shaped cable. Dimensions inside the figure are in meter, for example, the outer diameter is 47.5m meter(= 47.5mm)

the cores. In order to calculate them, one could resort to a Finite Element Method [FEM] program for the calculation, but the set up of such a FEM is tedious and requires knowledge of the FEM program.

Therefore a Caspoc [1] calculation tool is developed where the model is calculated from the geometrical data, see Fig. 3. Here the user enters the geometrical data for the cable on the left side of the screen in the input fields. The tool directly calculates the parameters of the circuit model that can be applied in the circuit simulation in Caspoc [1].

The geometric data is basically the cross-section of each core and the distance between the cores. From the cross-section of each core the core resistance is calculated. Temperature influences are taken care of according to [9].

$$R = R_{20}[1 + \alpha_{20}(T - 20)] \quad (7)$$

where:

- $R$  Conductor resistance at  $T$ [°C]
- $R_{20}$  Conductor resistance at 20[°C]
- $\alpha_{20}$  Temperature coefficient of resistance of the conductor material at 20[°C]
- $T$  Conductor temperature [°C]

In [9] there are also general formulas for calculating the inductance of a cable, however, this is too general to be applied here. For a correct calculation, the exact dimensions have to be known and entered into the tool, see Fig. 4. Based on the electromagnetic field distribution, the inductance per core and the magnetic coupling between each core is calculated. The dimensions are entered in [mm] and the geometrical data that has to be entered complies to the data usually given in a datasheet. For example, the sector width  $ws$  and sector depth  $ds$  are two common parameters for sector shaped core, see Fig. 4. Also the rounding of each core is of influence on the capacitive coupling between two neighboring cores and the

resistance of each core. The rounding's are specified as an equivalent radius for each corner, being  $R_{rcw}$  and  $R_{rcd}$ .

If the outer radius of the core  $rb$  and the insulation thickness  $t$  between two main cores is specified, the sector width  $ws$  and sector depth  $ds$  parameters are calculated by the tool based on  $rb$  and  $t$ . If  $t$  is set to zero, the insulation  $t$  between the cores is calculated by the tool based on the outer radius  $rb$  and the sector width  $ws$  and sector depth  $ds$ .

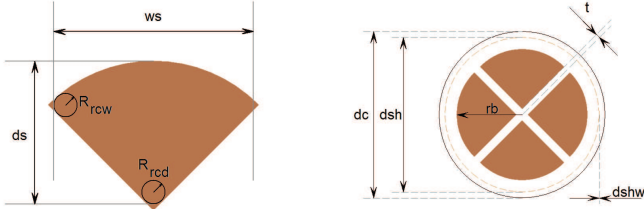


Fig. 4. Input of the geometry parameters for calculating the electrical parameters.

Since there are eight cores inside the cable, all electromagnetic coupling coefficients have to be calculated. Fig. 5 shows all possible coupling coefficients between a single main core and all other main cores, auxiliary cores and sheath using the solid arrows. The coupling coefficients between the auxiliary cores and sheath is indicated by the dashed arrows in Fig. 5.

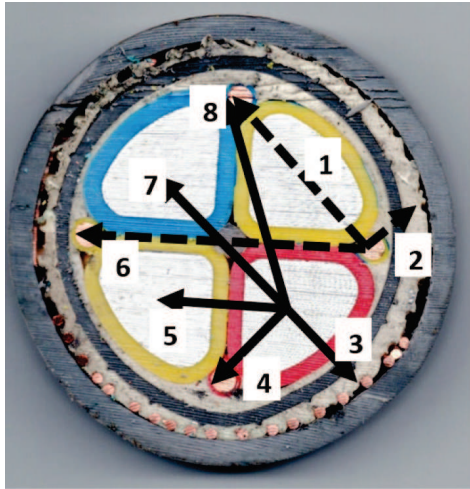


Fig. 5. Inductive coupling between the various wires inside the cable, the number indicates the index of the coupling.

The cores of the cable are divided among four main cores for the AC grid and four smaller auxiliary cores for the DC grid. Because of the sector shaped cores, the auxiliary cores are placed between two main cores. This means that an auxiliary core is always tightly coupled to only two main cores and loosely coupled to the other two main cores. This unbalance is also measured in the induced voltage as we shall see in the next section III.

The cores inside the cable have different coupling factors. Therefore the interface to the simulation model is configured such, that the connections to the model are exactly like in the

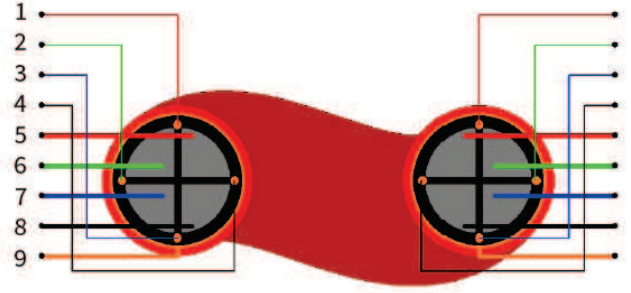


Fig. 6. Simulation model based on the calculated inductive and capacitive coupling

TABLE I  
CORE CONNECTIONS FROM FIG. 6

number	core type
(1)	Auxiliary core [Red]
(2)	Auxiliary core [Yellow]
(3)	Auxiliary core [Blue]
(4)	Auxiliary core [Blue/Yellow]
(5)	Main core [Red]
(6)	Main core [Yellow]
(7)	Main core [Blue]
(8)	Main core [Blue/Yellow]
(9)	Sheath

real cable. The numbers of the cores from Fig. 6 correspond to the numbers in the Table I.

In order to correctly apply the model in the simulation, each core has to be connected to the correct terminal. Since the electromagnetic coupling in Fig. 6 between core (5) and (6) is equal to the coupling between core (5) and (8) but it is completely different from the electromagnetic coupling between (5) and (7). Adjacent cores have a lower coupling factor, approximately 0.75 than the coupling between parallel cores, being approximately 0.8.

Also the coupling in Fig. 6 between auxiliary core (1) and cores (5) and (6) is much higher compared to the coupling to the other main cores (7) and (8).

Not surprisingly the capacitive coupling in Fig. 6 between the cores (5) and (6) is much higher than between the cores (5) and (7). The capacitive coupling between the cores (5) and (6) amounts considerably to the capacitive loading of the cable, while the capacitive coupling between the cores (5) and (7) can be nearly neglected. The capacitive coupling between all main cores and the sheath is also considerable and amount to the total capacitive loading of the cable.

In the tool from Fig. 3, all core inductances and mutual couplings are calculated as well as all capacitance between all cores, except those capacitance values small enough to be neglected. The resistance of each core is calculated and is temperature dependent. The parameters are inserted in the simulation model in Caspoc [1], where transient simulations based on the cable model can be performed.

The calculated parameters are compared with two measurements, [11] and [12] on The Green Village [10] and compared to the given parameters from the datasheet [8]. Calculated and

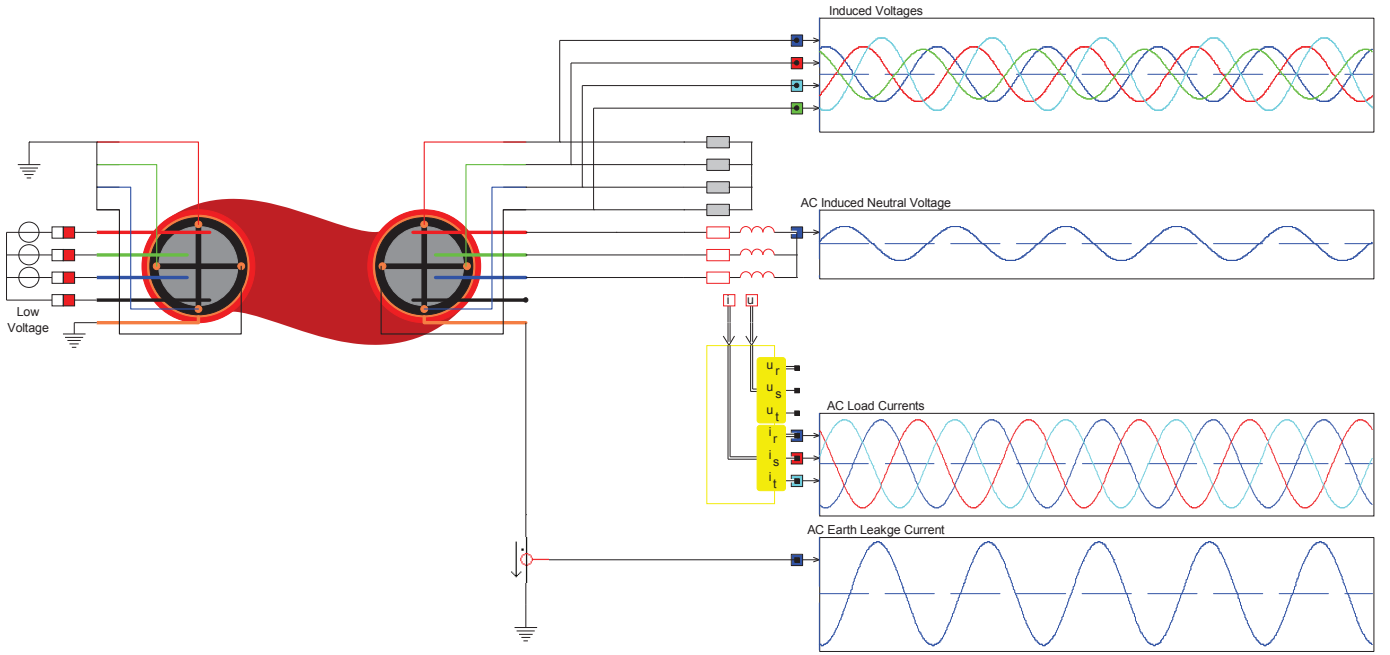


Fig. 7. Induced voltage on the auxiliary cores

measured core resistance are in close agreement, while the calculated loop inductance is in agreement with the datasheet inductance. Calculated and measured core inductance are in close agreement, but not given in the datasheet. From the calculated capacitance the nominal load capacitance is derived and is in close agreement with the specified nominal capacitance from the datasheet.

### III. CROSSTALK

Before starting with analyzing the performance of the cable in a larger system, it is advised to first understand the crosstalk inside the cable. To get a better understanding of the electromagnetic coupling between the cores inside the cable, we first look at the crosstalk of a single cable model.

In Fig. 7 a single cable segment is displayed. The main cores of the cable are connected to a 400V AC grid on the left side and on the right side the main cores of the cable are connected to an ohmic-inductive load of 30kW with a power factor equal to 0.9. The auxiliary cores on the left side of the cable are connected to earth, while on the right side they are loaded with constant resistors of 100Ω.

The upper scope shows the induced voltages on the auxiliary cores. As expected, because of the asymmetrical field distribution of the AC grid, not all voltages induced in the auxiliary cores are of the same phase and amplitude. Only the voltages of the two auxiliary cores that are between three main cores, show a phase shift of 120° and equal amplitude.

The second scope shows the neutral voltage of the AC load. Since there are four main cores, there is an asymmetrical field distribution inside the cable which causes a non-zero neutral voltage.

The third scope shows AC load currents. These are pure sinusoidal waveforms as we are having an ideal inductive load.

The last scope at the bottom shows earth-leakage current measured at the load side of the cable. Because of the asymmetrical field distribution inside the cable a current gets induced in the neutral core.

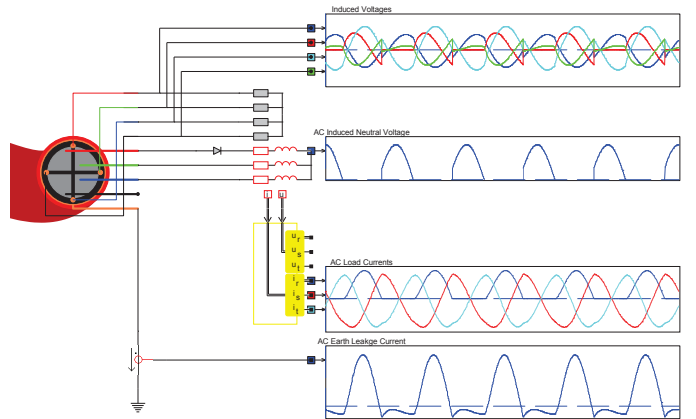


Fig. 8. Induced voltage on the auxiliary cores with asymmetrical AC load

In Fig. 8 the AC load is made non-linear by including a single diode. The result are induced harmonics on the auxiliary cores as can be seen in the upper scope in Fig. 8. From this simulation we can conclude that transient disturbances in the AC grid, that could occur because of faults in the AC grid, are directly coupled from the AC grid to the DC grid.

The DC grid is applied in Fig. 9, where the left side of the cable is connected to two ideal DC voltage sources of 350V each. The DC load is on the right side of the cable consisting

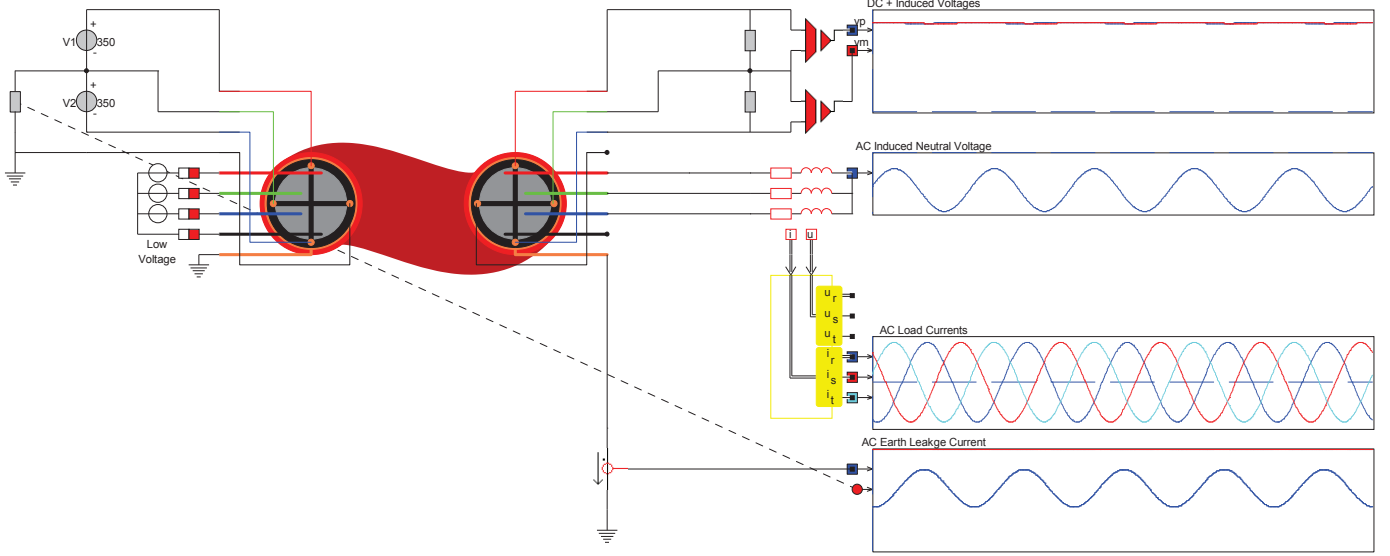


Fig. 9. Induced voltage on the auxiliary cores superimposed on the DC voltage

of two  $100\Omega$  resistors. The induced voltages on both loads are displayed in the upper scope and in Fig. 10. As expected the induced voltage is superimposed on the DC grid voltage.

Harmonics and disturbances occurring on the AC grid are thus coupled to the DC grid. Although these disturbances might seem small, they are measured by the protection systems on the DC grid. The amplitude of the induced harmonics and disturbances depends on the length of the cable. Each core has a self inductance of roughly [11]

$$L \equiv \frac{\mu_o}{2\pi} \cdot l \cdot \ln \frac{a}{r} \quad (8)$$

where

- $l$  is the core length[m],
- $a$  is the distance between two cores[m] and
- $r$  is the core radius[m].

The coupling is mainly defined by the mutual inductance between two cores

$$M \equiv 2 \cdot l \left\{ \ln\left(\frac{2l}{d}\right) - 1 + \frac{d}{l} \right\} \quad (9)$$

where

- $l$  is the core length[m] and
- $d$  is the core radius[m].

Any change in current in the AC grid is coupled via the mutual inductance  $M$  into the DC grid as

$$v_{DCgrid} = M \frac{di_{ACgrid}}{dt} \quad (10)$$

Therefore the induced voltage is higher for increasing cable length. The influence of the capacitive coupling between the main cores and the auxiliary cores is much lower with regard to coupling of induced faults and disturbances from the AC grid into the DC grid.

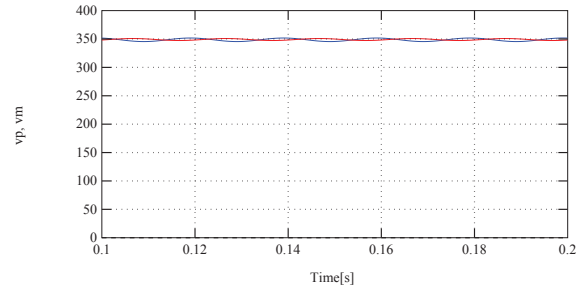


Fig. 10. 350V DC voltage with induced AC ripple voltage due to the induced AC load current, Voltage  $vp$  [Red] between the Positive[N] and Neutral[N] rail and  $vm$  [Blue] between the Neutral[N] and Negative[M] rail in [volt].

#### IV. PROTECTION

Earth-leakage and short-circuit protection are the two main protections methods that have to be implemented. Compared to protection in AC grids, there are two main advantages when using a DC grid:

- 1 Short-circuit protection does not need short-circuit power to detect short-circuit.
- 2 Earth-leakage measurement is possible even with longer cables and more lighting poles.

The short-circuit and earth-leakage protection are based on the measurement of an instantaneous change of current and measurement of the maximum current .

Since for the DC grid the core impedance only consists of core resistance and the voltage drop over the core inductance is close to zero, earth-leakage can be detected more easily and precise as compared to AC grids. Also since the capacitive

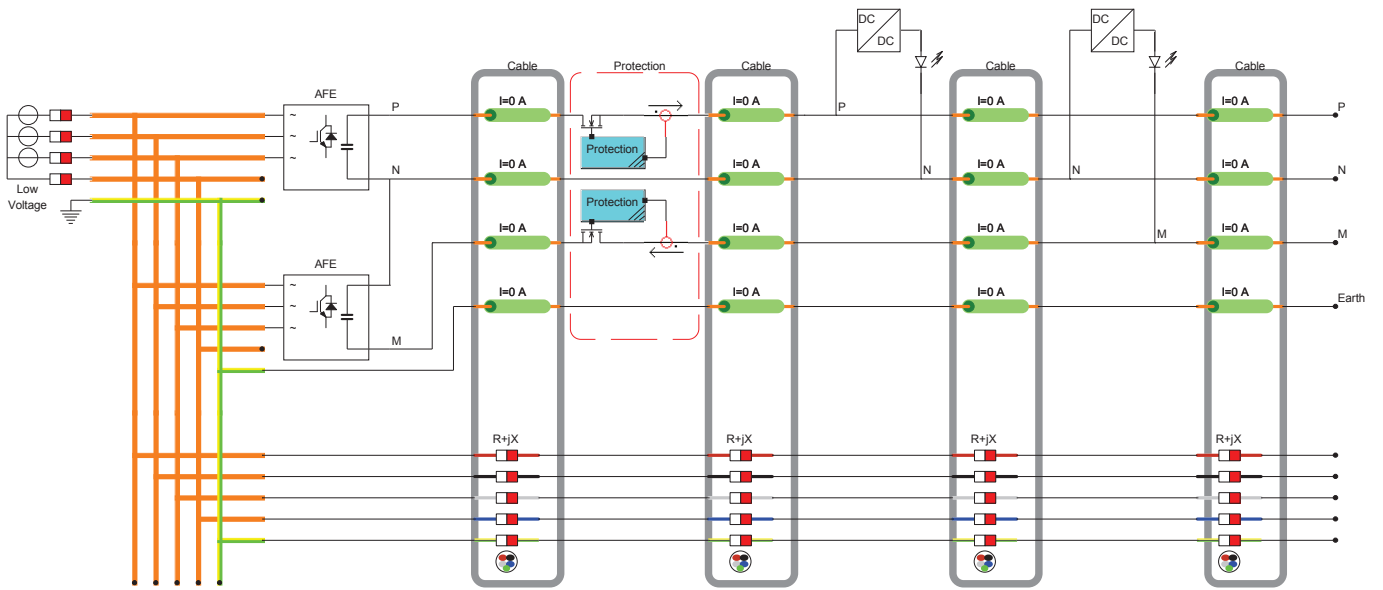


Fig. 11. DC distribution with earth-leakage and short-circuit protection.

coupling has no influence on earth-leakage in a DC grid, the earth-leakage current is easier to detect in case of a fault. This allows longer cables and still have the ability to detect earth-leakage.

Short-circuit protection is not only defined by the maximum current that is allowed before a circuit breaker switches off the load, but on the rise of the current. In [13] and [14] the change of current is measured and before the maximum current is reached, the circuit breaker switches off the load. This turning off can be within  $1ms$  for a  $700V$  DC grid, see [13].

In Fig. 11 two poles are connected to a DC grid with protection. From left to the right in Fig. 11 it starts with the low voltage  $400V$  three phase AC grid which is distributed towards two Active Front Ends [AFE]. The AFE's create a  $-350V \leftrightarrow 0V \leftrightarrow +350V$  DC grid and are able to control the power factor in the AC grid. By connecting two AFE's in series a total voltage of  $700V$  is created and distributed over three auxiliary cores of the combined-cable. The main cores of the combined-cable are connected the AC grid via the distributor.

The protection is placed in the DC grid on the positive and negative auxiliary core. Maximum current measurement and  $di/dt$  measurement is performed to track fault conditions. The current Router from [13] disconnects the DC grid when the current exceeds its maximum current and also disconnects if the increase in current exceeds a predefined slope of  $750kA/s$ .

Since the DC grid is a  $-350V \leftrightarrow 0V \leftrightarrow +350V$  the lighting poles are connected alternatively between the positive auxiliary core [P] and neutral auxiliary core [N] and between the neutral auxiliary core [N] and the negative(minus) auxiliary core [M]. Each lighting pole has a build in DC/DC converter for controlling the current through the LED strings and also the task of turning the light on and off remotely.

## V. CASE STUDY

At The Green Village [10] in Delft the first case study of a combined AC and DC grid using the combined-cable will be performed. A  $200m$  cable and 20 light poles are connected in a ring structure, see Fig. 12. The DC grid will be build using protection as shown in Fig. 11. The ring structure will feed 20 lighting poles of  $20W$  each and an extra  $200m$  meter of cable will be used to feed 4 lighting poles of  $400W$  each. To simulate the current distribution through the combined-cable, in Fig. 13, 12 lighting poles are connected to an AC grid loaded combined-cable [12].



Fig. 12. DC grid ring structure at The Green Village in Delft.

The induced voltage on the auxiliary cores has an amplitude of  $\pm 10$  volt as indicated in Fig. 14 [12]. This level is not influencing the protection system in the DC grid as confirmed by measurements in [11].

## CONCLUSIONS

Combining a DC grid for public lighting with an AC grid on a single combined-cable is feasible. A simulation model for the cable is set up and parametrized based on the geometrical

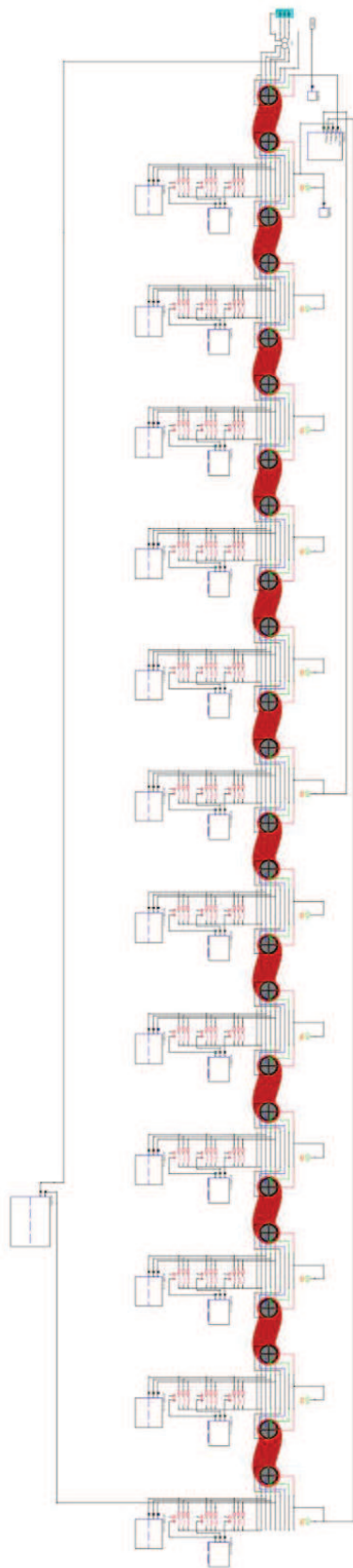


Fig. 13. Case study: Loaded AC grid and DC grid with 12 lighting poles.

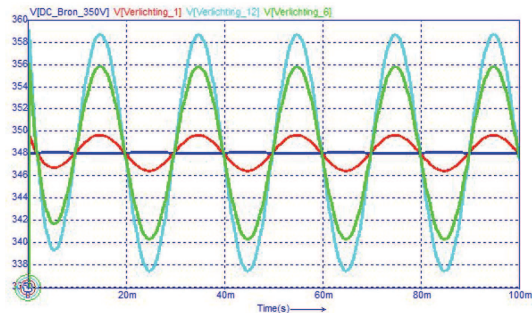


Fig. 14. Induced AC voltages on the 350V DC voltage due to crosstalk.

data of the cable. Simulations and experimental verification of the parameters of the cable are in close agreement and confirm given parameters from the datasheet. A case study to prove the combination of the AC grid and DC grid on the combined-cable will be carried out and experimental results prove the operation of a current router in the DC grid. Improvements are the reduced costs and reduced maintenance, on the business case side and earth-leakage detection as well as short-circuit detection with reduced power on the technical side.

#### REFERENCES

- [1] Caspoc, <http://www.caspoc.com>, 2017.
- [2] Mackay et al., From DC nano- and microgrids towards the universal DC distribution system - a plea to think further into the future, IEEE Power & Energy Society General Meeting, Denver, 2015, doi: 10.1109/PESGM.2015.7286469
- [3] D. Salomonsson, L. Soder and A. Sannino, "Protection of Low-Voltage DC Microgrids," in IEEE Transactions on Power Delivery, vol. 24, no. 3, pp. 1045-1053, July 2009., doi: 10.1109/TPWRD.2009.2016622
- [4] W. A. G. de Jager and P. J. Bos, "Design of a public DC grid of a business park," 2017 19th European Conference on Power Electronics and Applications (EPE'17 ECCE Europe), Warsaw, 2017, pp. P.1-P.9. doi: 10.23919/EPE17ECCEEurope.2017.8099272
- [5] M. Hulsebosch, P. Willigenburg, J. Woudstra and B. Groenewald, "Direct current in public lighting for improvement in LED performance and costs," 2014 International Conference on the Eleventh industrial and Commercial Use of Energy, Cape Town, 2014, pp. 1-9., doi: 10.1109/ICUE.2014.6904186
- [6] J. B. Woudstra, P. van Willigenburg, B. B. J. Groenewald, H. Stokman, S. De Jonge and S. Willems, "Direct current distribution grids and the road to its full potential," 2013 Proceedings of the 10th Industrial and Commercial Use of Energy Conference, Cape Town, 2013, pp. 1-7.
- [7] W. Aerts, S. Willems, D. Haeseldonckx, P. van Willigenburg, J. Woudstra and S. De Jonge, "Study and simulation of DC micro grid topologies in Caspoc," Twenty-Second Domestic Use of Energy, Cape Town, 2014, pp. 1-6., doi: 10.1109/DUE.2014.6827760
- [8] Twentse Kabelfabriek, V-VMvKhsas 0,6/1 kV NEN 3616, [www.tkf.nl](http://www.tkf.nl), 2018
- [9] BICC Cables Ltd., Electric Cables Handbook, 3rd Edition, Wiley-Blackwell, 1997
- [10] Green Village Delft Technical University, [www.thegreenvillage.org](http://www.thegreenvillage.org)
- [11] Belt et al., Eindrapport DC en AC door een combikabel, THUAS, 2018
- [12] de Jong et al., Wisselspanning en Gelijkspanning op de Combikabel, THUAS, 2018
- [13] Current Router, <https://www.directcurrent.eu/nl/producten/170-current-router>, DC current, 2018
- [14] DC-Grid Manager, <https://www.iisb.fraunhofer.de/>, Fraunhofer IISB, 2018